



UNIVERSITY OF LEEDS

This is a repository copy of *Peptide-Functionalized Quantum Dots for Rapid Label-Free Sensing of 2,4,6-Trinitrotoluene*.

White Rose Research Online URL for this paper:

<https://eprints.whiterose.ac.uk/159580/>

Version: Accepted Version

Article:

Komikawa, T, Tanaka, M, Tamang, A et al. (3 more authors) (2020) Peptide-Functionalized Quantum Dots for Rapid Label-Free Sensing of 2,4,6-Trinitrotoluene. *Bioconjugate Chemistry*. ISSN 1043-1802

<https://doi.org/10.1021/acs.bioconjchem.0c00117>

© 2020 American Chemical Society. This is an author produced version of an article published in *Bioconjugate Chemistry*. Uploaded in accordance with the publisher's self-archiving policy.

Reuse

Items deposited in White Rose Research Online are protected by copyright, with all rights reserved unless indicated otherwise. They may be downloaded and/or printed for private study, or other acts as permitted by national copyright laws. The publisher or other rights holders may allow further reproduction and re-use of the full text version. This is indicated by the licence information on the White Rose Research Online record for the item.

Takedown

If you consider content in White Rose Research Online to be in breach of UK law, please notify us by emailing eprints@whiterose.ac.uk including the URL of the record and the reason for the withdrawal request.



eprints@whiterose.ac.uk
<https://eprints.whiterose.ac.uk/>

1
2
3
4
5
6
7
8
9
10
11
12
13
14

Research Article

Peptide-Functionalized Quantum Dots for Rapid Label-Free Sensing of 2,4,6-Trinitrotoluene (TNT)

Takumi Komikawa,[†] Masayoshi Tanaka,[†] Abiral Tamang,[‡] Stephen D. Evans,[‡] Kevin Critchley,^{,‡} Mina Okochi^{*,†}*

[†]Department of Chemical Science and Engineering, Tokyo Institute of Technology, 2-12-1, Ookayama, Meguro-ku, Tokyo 152-8552, Japan

[‡]School of Physics and Astronomy, University of Leeds, Leeds LS2 9JT, United Kingdom

15 **ABSTRACT**

16 Explosive compounds, such as 2,4,6-trinitrotoluene (TNT), pose a great concern in terms of both
17 global public security and environmental protection. There are estimated to be hundreds of TNT
18 contaminated sites all over the world, which will affect the health of humans, wildlife and the
19 ecosystem. Clearly, the ability to detect TNT in soils, water supplies, and wastewater is important
20 for environmental studies, but also important for security, such as in ports and borders. However,
21 conventional spectroscopic detection is not practical for on-site sensing because it requires
22 sophisticated equipment and trained personnel. We report a rapid and simple chemical sensor for
23 TNT by using TNT binding peptides which are conjugated to fluorescent CdTe/CdS quantum dots
24 (QDs). QDs were synthesized in the aqueous-phase and peptide was attached directly to the surface
25 of the QDs by using thiol groups. The fluorescent emission from the QDs was quenched in
26 response to the addition of TNT. The response could even be observed by the naked-eye. The limit
27 of detection from fluorescence spectroscopic measurement was estimated to be approximately 375
28 nM. In addition to the rapid response (within a few seconds), selective detection was demonstrated.
29 We believe this label-free chemical sensor contributes to progress the on-site explosive sensing.

30

31 **KEYWORDS**

32

33 Peptide, Quantum dots, Explosive detection, Fluorescence chemical sensor

34

35

36 INTRODUCTION

37

38 Explosive detection has become important from the viewpoint of worldwide public security and
39 food safety. 2,4,6-Trinitrotoluene (TNT) is one of the most commonly used nitroaromatic
40 compounds for military purposes. It also causes serious contamination in ground soil and drinking
41 water when leaked from landmines and weapons¹. To date, various types of laboratory-based
42 studies have been reported to achieve highly-sensitive and specific detection of TNT using
43 conventional analytical methods (e.g. gas-chromatography mass-spectrometry (GC/MS), Fourier-
44 transformed infrared spectroscopy and Raman spectroscopy)²⁻⁶. However, these techniques are
45 difficult to apply to on-site sensing because they demand time-consuming and costly sample
46 preparation. In addition, the subsequent processes of detection and analysis, require sophisticated
47 equipment as well as trained personnel. For practical uses, especially at the places such as a
48 minefield or security control in an airport, the sensing devices are required to be sensitive, specific,
49 easy-to-use, inexpensive, and rapid. Several novel approaches including fluorescence chemical
50 sensor, surface plasmon resonance (SPR), and electrochemical sensors may potentially be
51 applicable to on-site explosive detection⁷⁻¹⁰. Among these, the fluorescence-based methods are
52 attractive because only easy-handling and simple equipment is required (e.g. a light detector and
53 a light source). The quenching of molecular probe-functionalized metal quantum dots (QDs)
54 caused by energy transfer or electron transfer¹¹⁻¹³ and inner filter effect of carbon QDs or silicon
55 nanoparticles were previously utilized for the explosive detection^{14,15}. In addition, as other
56 fluorescence materials, metal organic frameworks or nonporous polymers were also used^{16,17}.
57 However, from the viewpoint of the applicability for versatile types of target molecules and the

58 simplicity of the material preparation, QDs covalently functionalized with target recognition probe
59 are promising materials for the detection.

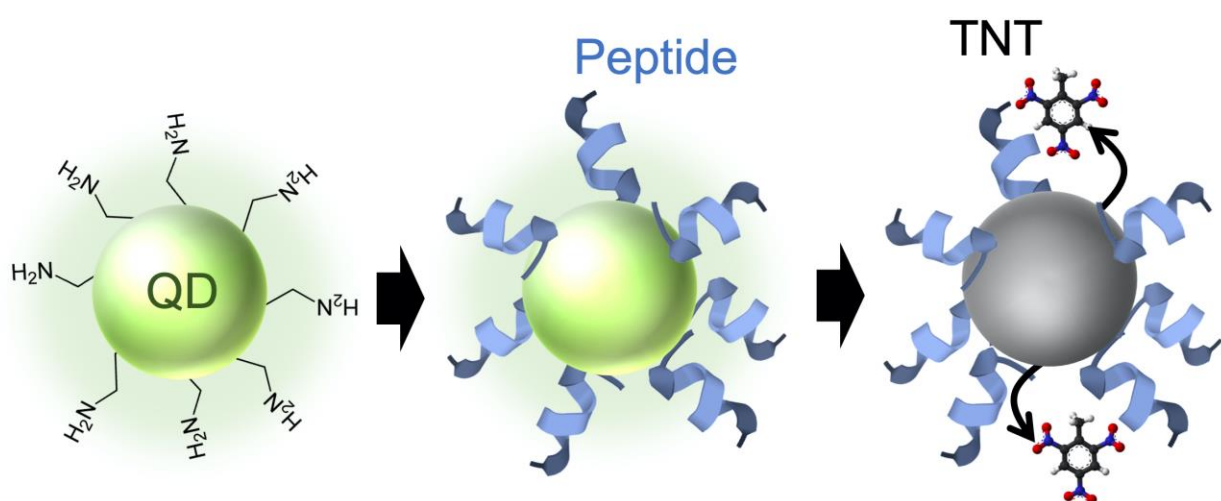
60 For the selective entrapment and detection of small analyte, TNT, molecular recognition probes
61 such as antibody-based recombinant proteins, peptides, or molecular imprinted polymers (MIP)
62 were immobilized on the particle surface. In some cases, a pattern analysis technique is used to
63 support the target determination among similar compounds^{11-13,18,19}. Although antibody
64 recombinant proteins, such as single-chain variable fragments, could perform specific binding
65 properties to target molecules, they have some shortcomings related to the complicated production
66 process requiring microorganisms or animal cells, and careful storage. Some researchers took
67 advantage of MIP integrated with gold nanoparticles (AuNPs) for TNT detection; or the
68 combination of MIP and DNA aptamers for enhancing both the sensitivity and selectivity^{20,21}. In
69 terms of direct binding, ease-of-synthesis, and stability, a chemically synthesized peptide is one of
70 the promising probes for capturing a target molecule^{22,23}.

71 In previous studies, we produced an anti-TNT antibody²⁴ and screened TNT binding peptides
72 from the complementarity-determining regions (CDRs) of the antibody²⁵. CDRs are paratope sites
73 in a variable region of antibody and three CDRs each exist in both light chain and heavy chain.
74 Through the comparative TNT binding assay using these six CDRs, the heavy chain CDR3
75 (HCDR3) peptide was determined to be the strongest binder to TNT. The core 12-mer TNT binding
76 peptide (TNT-BP, ARGYSSFIYWFF) was discovered by the optimization among a series of
77 truncated sequences of HCDR3²⁵. This TNT-BP was applied to SPR-based TNT detectors, and
78 sensitive and selective detection of TNT was demonstrated^{26,27}.

79 Herein, toward further development of simple and rapid detection system, fluorescence detection
80 system using peptide-functionalized QDs was investigated. A new material (TNT-BP-C@QDs)

81 for TNT sensing comprising TNT-BP-C (TNT-BP supplemented cysteine at C-terminus) modified
82 CdTe/CdS core/shell QDs was designed and was used as a TNT detector owing to its fluorescence
83 quenching ability in the presence of TNT (Figure 1). We believe this technique encourages the
84 development of rapid, simple, selective and low-cost on-site explosive detection in various fields.

85
86
87



88
89 **Figure 1** Schematic illustration of fluorescent quench detection by TNT with TNT-BP-C immobilized
90 CdTe/CdS QDs.

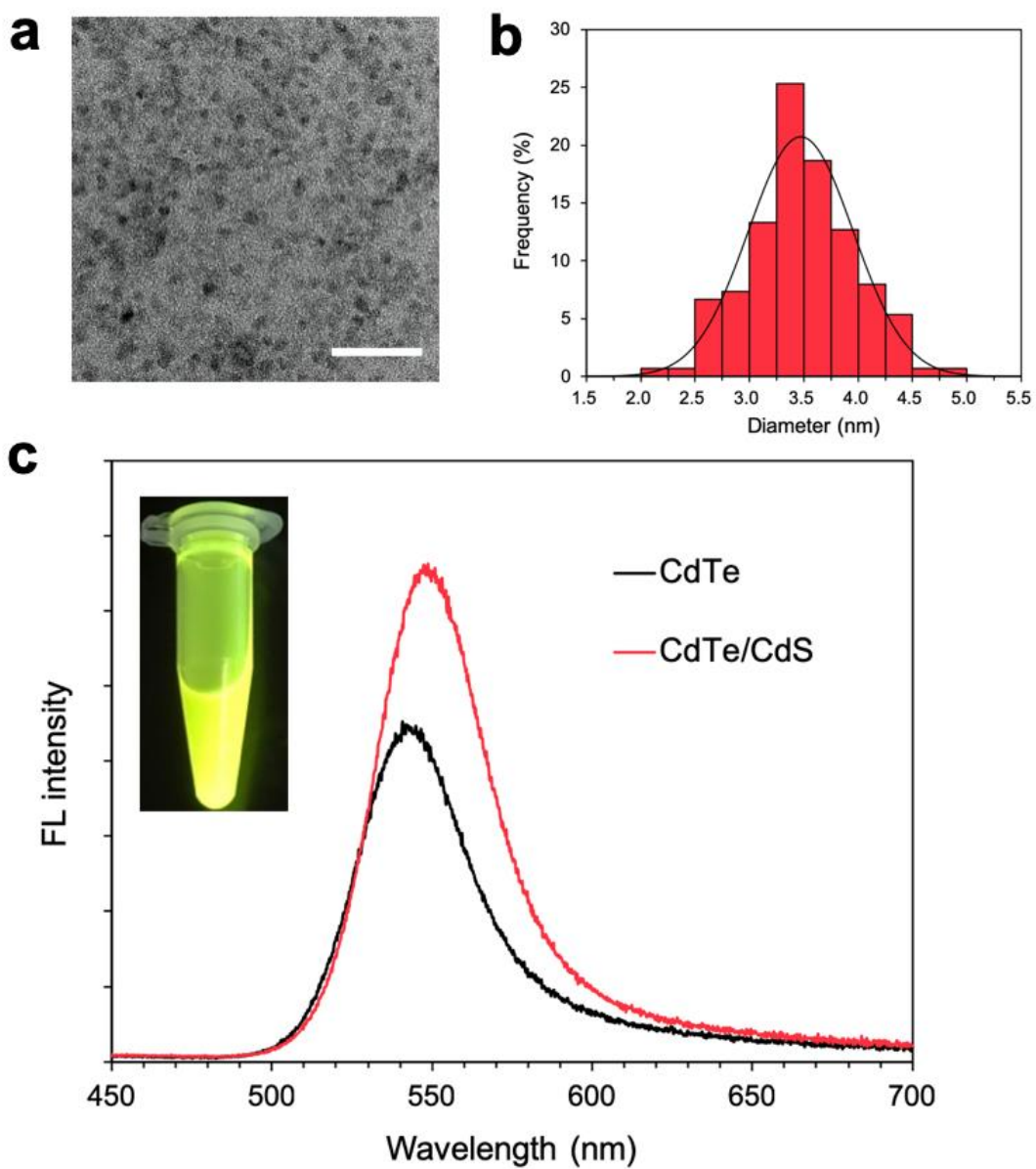
91

92 **RESULTS AND DISCUSSION**

93

94 **Preparation of CdTe/CdS QDs**

95 CdTe/CdS QDs were prepared following aqueous phase method and the fluorescence emission
96 and PLQY (photoluminescence quantum yield) were measured. A high-resolution transmission
97 electron microscope (HR-TEM) image of the synthesized CdTe/CdS QDs is shown in Figure 2a.
98 The histogram of the QD size distribution was obtained by analyzing 200 particles (Figure 2b).
99 The mean and standard deviation of the QD diameters were determined by fitting a normal
100 distribution, which resulted in 3.5 ± 0.5 nm. The fluorescence emission spectra of core CdTe and
101 CdTe/CdS QDs were measured by fluorescence spectroscopy (Figure 2c). Both of them emitted
102 greenish-yellow fluorescence and the peak wavelength was red-shifted (from 546 nm to 551 nm)
103 after shell coverage. The PLQYs of core and core/shell QDs were measured to be 8.5% and 11.3%,
104 respectively. The PLQY of these samples are much lower than typically synthesized QDs for
105 which thioglycolic acid is used as the stabilizing ligand. This suggests that the CdS shell growth
106 using thiourea is not as effective at passivating surface trap states when cysteamine is used to coat
107 the QDs.



108
 109 **Figure 2** **a** Microscopic observation of synthesized CdTe/CdS QDs by HR-TEM (scale bar: 30 nm). **b**
 110 Size distribution of QDs obtained from TEM images. Mean particle diameter is calculated to be 3.5 ± 0.5
 111 nm. **c** Fluorescence spectra of QDs before and after CdS shell coverage. The inset shows the optical
 112 image of CdTe/CdS core/shell QDs under UV-lamp.

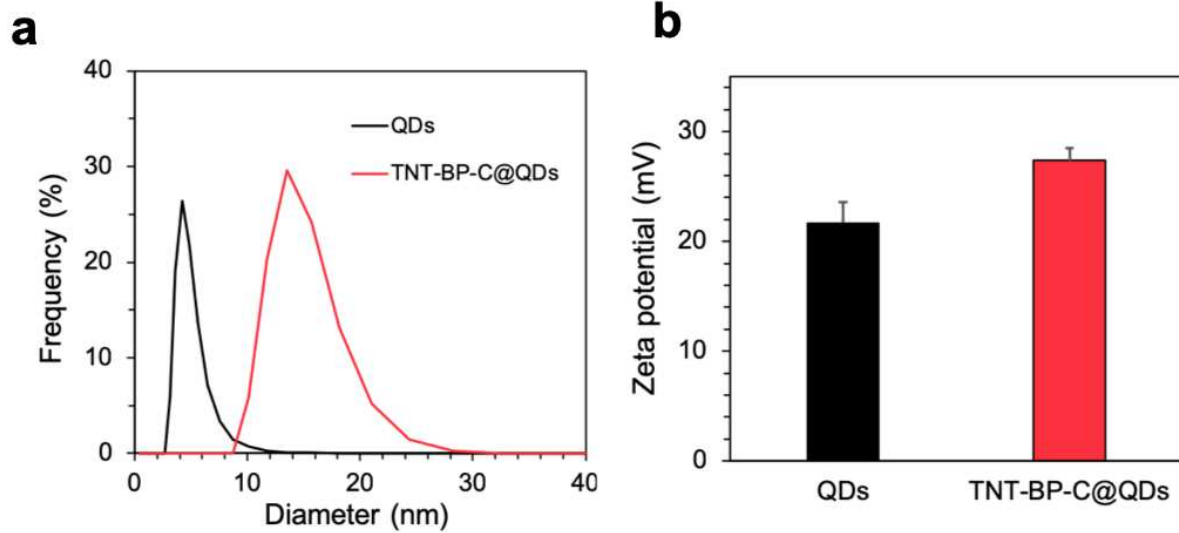
113
 114

115 **Fabrication and characterization of TNT-BP-C@QDs**

116 Prior to the experimental evaluation of TNT binding, the QD functionalization condition was
117 optimized by using different peptide concentration including, peptide:QD = 5:1, 10:1 and 20:1 for
118 overnight. As the result, when the peptides were modified at the condition of 20:1, the aggregation
119 of QDs with lower fluorescent intensity was observed. This is probably because the ligand
120 exchange from cysteamine to cysteine tagged peptide (TNT-BP-C) caused side effect to the
121 particle dispersibility. Based on the evaluation, the peptide modification was conducted at the
122 condition of peptide:QD=10:1 in this study.

123 TNT-BP-C was synthesized following standard Fmoc-based protocol and immobilized on the
124 surface of CdTe/CdS QDs via the thiol group. After overnight stirring of the mixture of TNT-BP-
125 C and QDs, the peptide modification was confirmed by an increase in mean hydrodynamic
126 diameter (Figure 3a) and a change in zeta potential that was shifted to a higher positive value
127 (Figure 3b). Qualitatively, this can be understood because the peptide is positively charged (pI:
128 8.8). After peptide binding, the fluorescence emission peak was found to slightly blue-shifted
129 (Figure S1). TNT-BP-C@QDs can be synthesized easily. In addition to the material synthesis
130 process, this detection method is no-need of both expensive equipment and highly trained
131 personnel, thus the sensing system is cost-effective compared to the conventional detection
132 techniques (e.g. GC/MS or HPLC).

133



134

135 **Figure 3** Optical diameter distribution change measured by dynamic light scattering (**a**) and zeta

136 potential shift (**b**) before and after TNT-BP-C immobilization on CdTe/CdS QDs.

137

138

139

140 **Fluorescence quench detection of TNT by TNT-BP-C@QDs**

141 The fluorescent emission intensity of the TNT-BP-C@QDs was found to decrease in response
142 to increasing TNT concentration (Figure 4a). The emission was almost 70% lower than initial
143 intensity at the highest concentration of TNT added (90 μM). Then, the emission intensity, at the
144 peak maxima of 560 nm, was measured against TNT concentration in Figure 4b. For making Stern
145 Volmer plot, $(I_0/I)-1$, which indicates relative quenching of measured intensity (I) from the initial
146 value (I_0), were plotted against TNT concentration, [TNT]. There is a linear relationship ($R^2=0.97$)
147 in higher range (3-100 μM) of TNT concentration and the quenching coefficient, K_{sv} is estimated
148 to $3.2 \times 10^4 \text{ M}^{-1}$. This K_{sv} value is comparable with previously reported fluorescence-based
149 explosive sensors (Table S1). Whereas, Stern-Volmer equation does not provide a good fit to the
150 experimental data in lower concentration range. This is possibly because the limited access of the
151 quencher caused the downwards trend of plot. In addition, the fluorescence lifetime measurement
152 was conducted with different TNT concentration. As shown in Figure S2, significant change of
153 fluorescence lifetime from 16.0 to 9.3 ns was observed before and after addition of TNT, which
154 indicates that the TNT molecules chemically interacting with the peptide probe on the QDs surface
155 and caused quench by energy transfer as a dominant quench mechanism. However, as the induction
156 of QDs aggregation is also a possible theory and several mechanisms can be involved at the same
157 time, further study is needed for clarifying the detailed quench mechanism.

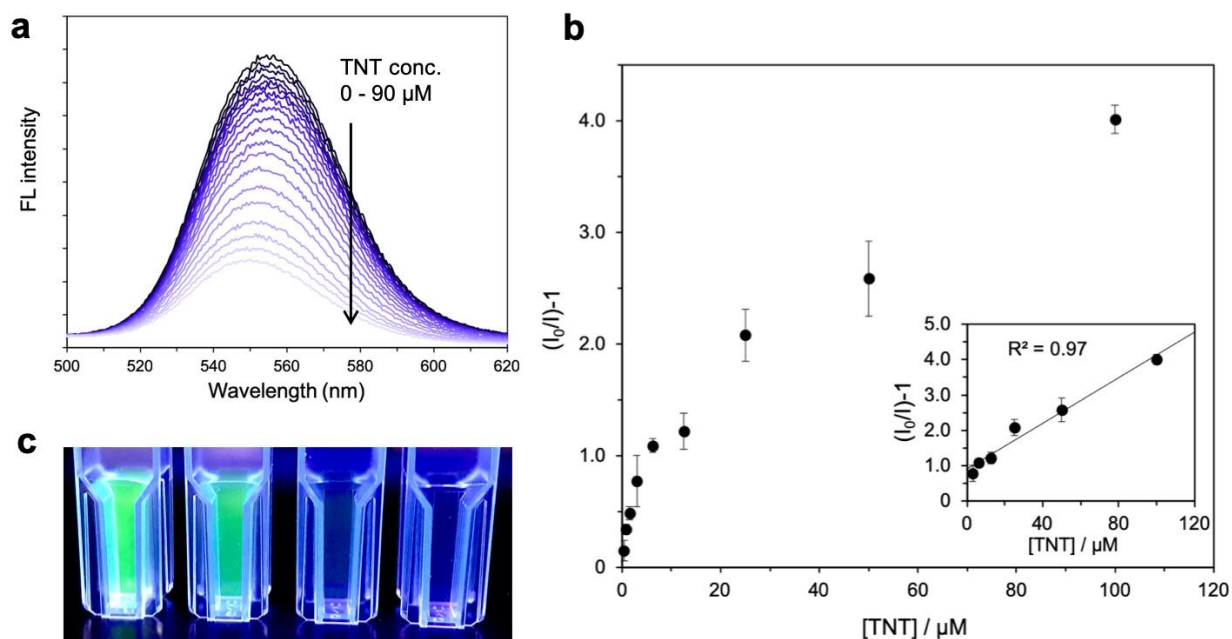
158 To determine the limit of detection, the fluorescence intensity was plotted against TNT
159 concentration (Figure S3). As this graph shows, the limit of detection (LOD) was 375 nM, which
160 is 1.5 times higher than the concentration of donor QDs (250 nM). Although the limit of detection
161 is required to be further improved, it is considered that the LOD depends on the QDs concentration

162 and there is a possibility to improve LOD by using another QDs with higher PLQY or more
163 sensitive FL detector.

164 When it comes to the practical uses, the simplicity of detection can be as important as the
165 detection sensitivity. Under the luminescence of UV lamp, the fluorescence quench in response to
166 the amount of TNT was observed by naked-eye in relatively higher concentrations ($>50 \mu\text{M}$)
167 (Figure 4c). This is promising for easy-to-use and on-site detection at the scene of requiring
168 detection without any other equipment and preparation.

169

170



171

172 **Figure 4 a** Representative fluorescence spectra of 100 nM TNT-BP-C@QDs solution in response to
173 increasing concentration of TNT. **b** $(I_0/I)-1$ is plotted as a function of TNT concentration for confirming
174 the Stern-Volmer equation. The linear dynamic range of Stern-Volmer plot is estimated to 3-100 μM
175 (inlet). **c** The optical image of 250 nM TNT-BP-C@QDs under UV-lamp with 0, 50, 100, 200 μM of
176 TNT, respectively, from left to right.

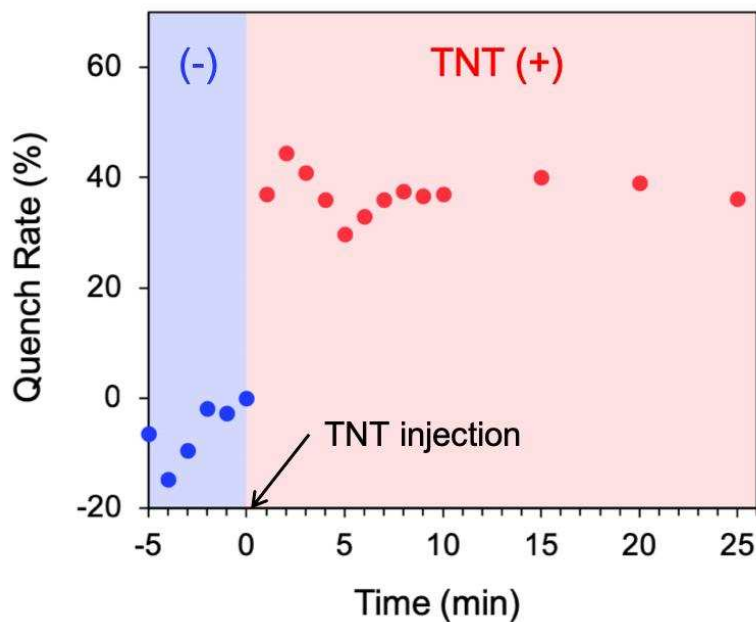
177 **Rapid and selective detection of TNT**

178 The reaction time is also an important parameter for the chemical sensing, and both shorter
179 response time and longer duration are preferable. The result in Figure 5 shows the quench rate,
180 which stands for $1-(I/I_0)$, at each time point before and after the injection of TNT to TNT-BP-
181 C@QDs solution. From this result, fluorescence quenching occurred within 1 min and was
182 maintained for at least 30 min after starting reaction. This quick reaction phenomenon is further
183 demonstrated in Supplementary Movie 1, and it is observed that the fluorescence emission was
184 rapidly quenched by addition of TNT sample within a few seconds. Thus, this quench-based TNT
185 detection has a great advantage in rapidity and simplicity for the on-site practical uses.

186 Furthermore, to evaluate the selectivity of TNT detection by TNT-BP-C@QDs, 2,4-
187 dinitrotoluene (DNT), 2,6-DNT, 2-nitrotoluene (NT), toluene and amyl nitrate were used as TNT
188 analogues. 2,4-DNT, 2,6-DNT and 2-NT were selected as representatives with aromatic ring and
189 different number of nitro groups. Toluene was chosen as a representative of non-nitro aromatic
190 compounds and amyl nitrate was selected as a non-aromatic nitro compound. To evaluate the
191 selectivity property of the developed material, the quench rate for each analyte at the same
192 concentration (100 μ M) is shown in Figure 6. The responses to toluene and amyl nitrate were more
193 than 3-fold lower than that to TNT. Whereas, 2,4-DNT, 2,6-DNT and 2-NT showed relatively
194 higher response than toluene. The number and position of nitro groups were suggested to have
195 important role for the binding between TNT-BP-C@QDs and analytes. TNT-BP was considered
196 to have specificity for TNT attributed to both its aromatic and basic amino acid residues, promoting
197 π -electron interaction and electrostatic interaction, respectively. Also this specific binding
198 property was consistent with previous studies using an array-based and SPR-based TNT binding
199 assay^{25,26}. Thus, these results affirm that the molecular recognition property of peptide probe has

200 been maintained on QDs. Although, other military explosives such as picric acid or 1,3,5-
201 Trinitroperhydro-1,3,5-triazine (RDX) should be tested in the future, this material could contribute
202 to selectivity of fluorescence quench-based TNT detection. In addition, through further
203 optimization of TNT detection condition (e.g. QD concentration), the selectivity and sensitivity
204 will be improved in the future.

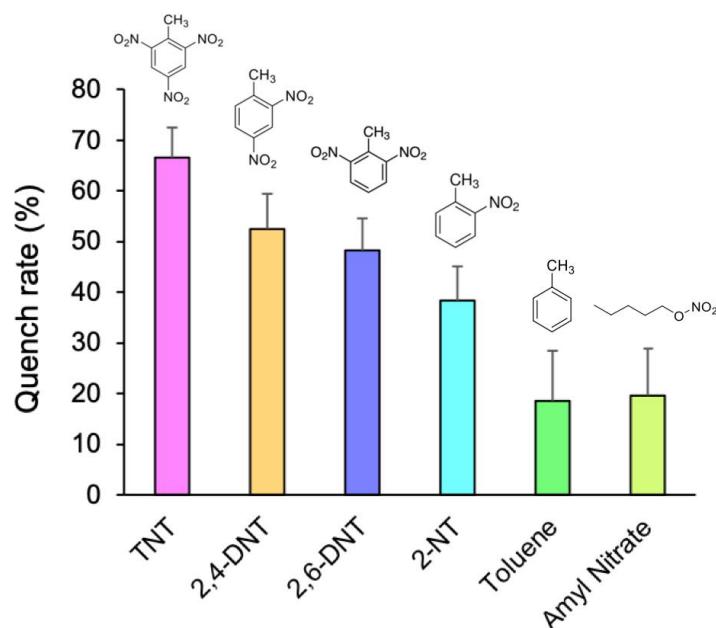
205



206

207 **Figure 5** The quench rate, $1-(I/I_0)$, of 100 nM TNT-BP-C@QDs is plotted as a function of time before
208 and after the injection of 50 μ M of TNT.

209



210

211 **Figure 6** Selectivity assay with 2,4-DNT 2,6-DNT, 2-NT, toluene and amyl nitrate. 100 μ M of analyte was
 212 added to 250 nM TNT-BP-C@QDs.
 213

214 The developed technique of a rapid and simple chemical sensor for TNT could be applied to on
 215 site explosive detection. Especially, as the TNT samples utilized in this study contains acetonitrile
 216 derived from purchased TNT reagent, the wipe test of contaminated surface seems to suite in
 217 practical use. For further challenging samples (e.g. soil, air, and water-based environments),
 218 various sample dependent optimization of the detection parameters with sample preparation should
 219 be addressed. It should be also noted that the development of one-pot QD functionalization process
 220 would be able to improve the sensor stability, although the prepared functionalized QD is also
 221 stable for more than a week.

222 Herein, as the peptide function expression on nanoparticle surface was confirmed, the peptide
 223 probe would also function on other nanoparticles utilized for other applications. The functionalized
 224 magnetic nanoparticle may be useful for the magnetic recovery of TNT from contaminated
 225 samples. Furthermore, using plasmonic nanoparticles such as gold and silver nanoparticles, there

226 is a potential to develop the colorimetric sensor, which can determine by naked eye without any
227 light irradiation. In that case, the fluorescent quenching mechanism by the binding with TNT and
228 peptide-QD should be elucidated.

229

230 **CONCLUSION**

231 In this research, we demonstrated a rapid, selective and easy-to-use chemosensor material, TNT-
232 BP-C@QDs for TNT. TNT-BP selected from antibody paratope region was chemically
233 synthesized and conjugated CdTe/CdS QDs via thiol ligand exchange reaction without
234 complicated procedure or other materials. The fluorescence emission of this material
235 proportionally decreased depending on the concentration of TNT. The linear dynamic range and the
236 limit of detection were estimated to 3-100 μM and 375 nM, respectively, and simple detection by
237 naked-eye was also attained under UV-lamp irradiation. In addition, the response time was
238 confirmed to be less than 1 min and the specific response to TNT was affirmed. The rapid and
239 selective response property of this material was an attractive candidate for novel chemosensor in
240 various fields including on-site explosive detection.

241

242 **EXPERIMENTAL PROCEDURES**

243 **Reagents**

244 All chemicals studied were analytical grade. TentaGel Resin (capacity: 0.25 mmol g⁻¹) was
245 purchased from Intavis AG (Cologne, Germany). N-Fluorenyl-9-methoxycarbonyl (Fmoc)
246 protected L-amino acids, *O*-benzotriazole-*N,N,N',N'*-tetra-methyl-uronium-hexafluoro-phosphate
247 (HBTU), diisopropylethylamine (DIEA), trifluoroacetic acid (TFA), triisopropylsilane (TIPS),
248 *N,N*-dimethylformamide (DMF) and 20% piperidine solution in DMF were obtained from
249 Watanabe Chemical Ind., Ltd. (Hiroshima, Japan). Dichloromethane (DCM), ethanol, diethyl ether,
250 acetonitrile, 1-methyl-2-pyrrolidone (NMP), toluene and acetonitrile were purchased from
251 FUJIFILM Wako Pure Chemical Corp. (Osaka, Japan). TNT solution solution (1mg mL⁻¹ in
252 acetonitrile), 2-propanol, sodium hydrate, cadmium perchlorate hydrate, cysteamine and thiourea
253 were purchased from Sigma-Aldrich (St. Louis, USA). Aluminum telluride were provided from
254 ABSCO Limited (Haverhill, UK) and stored under N₂ atmosphere. Sulfuric acid was purchased
255 from Fisher Scientific (Loughborough, UK). 1,2-Ethanedithiol (EDT), thioanisole, 2,4-
256 Dinitrotoluene (2,4-DNT), 2,6-dinitrotoluene (2,6-DNT), 2-nitrotoluene (2-NT) and amyl nitrate
257 were purchased from Tokyo Chemical Industry Co., Ltd. (Tokyo, Japan). All aqueous solutions
258 were prepared with MilliQ grade deionized water.

259

260 **Preparation of TNT-BP-C**

261 The sequence of 12-mer TNT binding peptide (TNT-BP, ARGYSSFIYWFF) was previously
262 screened and optimized from the complementarity determining regions of anti-TNT antibody²⁵.
263 Cysteine residues were added to the C-terminus of the peptide sequence (TNT-BP-C,
264 ARGYSSFIYWF²⁵FC) to enable the immobilization of the peptide to the QD surface via thiol

265 coupling. The peptide was synthesized following the standard Fmoc-based solid-phase protocol
266 with Resprep SL automatic peptide synthesizer (Intavis AG, Germany). Briefly, Fmoc protected
267 amino acid residues were applied to the TentaGel Resin by stepwise for elongation of peptide
268 chain. The synthesized peptide was deprotected by 20% piperidine in DMF and cleaved from the
269 scaffold resin by the cleavage cocktail containing TFA, water, thioanisole, phenol, EDT and TIPS
270 (82.5:5:5:2.5:1). The peptides were precipitated in cold diethyl ether and dissolved in 30%
271 acetonitrile for the storage in a form of freeze-dried powder. Purification was performed by ODS-
272 80TS column (Tosoh Corp., Tokyo, Japan) and the high-performance liquid chromatography
273 (HPLC) system (LC-20AR, CBM-20A, SIL-20AC, CTO-20AC, SPD-20AV, Shimadzu Corp.,
274 Kyoto, Japan) before measuring the molecular weight by matrix assisted laser desorption /
275 ionization mass spectrometry (AXIMA-CFRPlus, Shimadzu Corp.) (Figure S1a). The final purity
276 of the peptide was confirmed to be >85% by ODS-100Z column (Tosoh Corp.) and the HPLC
277 system (Shimadzu Corp.) (Figure S1b).

278

279 **Synthesis and characterization of CdTe/CdS QDs**

280 Core CdTe QDs were prepared following a previously reported protocol²⁸. Briefly, 0.985 g of
281 Cd(ClO₄)₂·6H₂O and 0.488 g of cysteamine were dissolved in 100 mL of MilliQ water, and the
282 pH was adjusted to 5.6 by dropwise addition of 1 M sodium hydroxide. The solution was placed
283 into a three-neck flask with N₂ bubbling through it to remove oxygen. The core precursor synthesis
284 was initiated by injection of H₂Te gas provided by adding 20 mL of 1 M sulfuric acid to 200 mg
285 aluminum telluride powder in separate three-neck-flask which is connected by tubing. CdTe
286 nanocrystal growth was achieved by refluxing at 100 °C for 30 minutes. 200 mg of thiourea was
287 dissolved in 1.5 mL MilliQ and added to the QDs solution in three times (0.5 mL each) with an

288 interval of 1 min under refluxing for CdS shell growth. The QDs were cleaned by dialysis with
289 Mini dialysis kit 8 kDa (GE Healthcare, Chicago, USA) for 2 h just before use.

290 UV-vis. absorption spectra and photoluminescence emission spectra were recorded by Cary
291 5000 UV/Vis/NIR (Agilent, Cheadle, UK) and FLS1000 Photoluminescence Spectrometer
292 (Edinburgh Instruments, Edinburgh, UK), respectively. The photoluminescence quantum yield
293 (PLQY) and fluorescence lifetime were also measured by the FLS1000 Photoluminescence
294 Spectrometer with the integrating sphere accessory. To obtain the size distribution, CdTe/CdS QDs
295 were observed by high resolution transmission electron microscope (HR-TEM) FEI Tecnai T20
296 (FEI company, Oregon, USA). Dynamic Light Scattering (DLS) analysis and zeta potential
297 measurements were performed using Malvin Zetasizer Nano (Malvin, UK).

298

299 **Preparation of TNT-BP-C@QDs by immobilization of peptide on QDs surface**

300 The concentration of the CdTe/CdS QDs were determined using the previously reported
301 extinction coefficient-based method ²⁹. The QDs solution was diluted to 1 μ M with deionized
302 water and then mixed with 10 μ M TNT-BP-C peptide solution before being incubated overnight
303 in the dark at room temperature. The TNT-BP-C peptide, having a thiol group on the side chain of
304 its C-terminus residue, can be immobilized on the CdS shell by thiol ligand exchange reaction.
305 After peptide conjugation, excess peptide molecules were removed with Mini dialysis kit 8 kDa
306 (GE Healthcare, Chicago, USA).

307 To confirm the peptide modification, the zeta potential and the hydrodynamic diameters were
308 analyzed before, and after, conjugating peptide ligands. For the zeta-potential measurement, TNT-
309 BP-C@QDs were diluted to 100 nM with 1 mM sodium chloride solution. The mean of three
310 experiments is reported.

311
312
313
314
315
316
317
318
319
320
321
322
323
324
325
326
327
328
329
330
331

TNT detection assay by fluorescence quenching using TNT-BP-C@QDs

The fluorescence spectroscopic measurements for obtaining QDs spectra were performed with the sample in a disposable cuvette. TNT-BP-C@QDs were diluted to 100 nM with deionized water and TNT solution was added and mixed by pipetting. Fluorescence emission spectra with 380 nm excitation were acquired by the FLS1000 Photoluminescence Spectrometer. For estimating the limit of detection and selectivity for TNT, POWERSCAN 4 micro plate reader (DS Pharma Biomedical, Osaka, Japan) was also used. The TNT-BP-C@QDs were adjusted to a concentration of 250 nM and added to a 96 well-plate. Fluorescence emission intensity at 560 nm were measured at the excitation wavelength of 380 nm. The optical images of the quenching using concentrations of 0, 50, 100, 200 μ M of TNT were taken with 250 nM of TNT-BP-C@QDs under the luminescence of UV-lamp. The optical movie of 1 μ M TNT-BP-C@QDs mixed with 200 μ M TNT was filmed under UV-lamp by XT-20 camera (Fujifilm, Tokyo, Japan). The response time measurement was also performed in a cuvette and each intensity was measured at each time point for 30 min after the addition of TNT by FLS1000 spectrometer. For the TNT selectivity assay, 100 μ M of 2,4-DNT, 2,6-DNT, 2-NT, toluene and amyl nitrate were used as control analytes and performed by POWERSCAN 4 micro plate reader.

332 **ASSOCIATED CONTENT**

333 **Supporting Information**

334 The Supporting Information is available free of charge on the ACS Publications website at

335 DOI: XXX.

336 Fluorescence spectra of synthesized QDs before and after peptide conjugation,

337 Calibration curve for TNT detection, Characterization of TNT-BP-C, Movie of rapid

338 fluorescence quench of TNT-BP-C@QDs

339

340 **AUTHOR INFORMATION**

341 **Corresponding Authors**

342 *E-mail: K.Critchley@leeds.ac.uk, Phone: (+44)-113-343-3873.

343 *E-mail: okochi.m.aa@m.titech.ac.jp, Phone: (+81)-3-5734-2116.

344

345 **ORCID**

346 Masayoshi Tanaka: 0000-0002-4701-5352

347 Stephen D. Evans: 0000-0001-8342-5335

348 Kevin Critchley: 0000-0002-0112-8626

349 Mina Okochi: 0000-0002-1727-2948

350

351 **Notes**

352 The authors declare no competing financial interest.

353

354 **ACKNOWLEDGMENT**

355 This work was supported by Cross-ministerial Strategic Innovation Promotion (SIP) Program
356 and Impulsing Paradigm Change through Disruptive Technologies (ImPACT) Program (Cabinet
357 Office, Government of Japan) and the international collaboration research projects (the JSPS and
358 the Royal Society) (IEC/R3/170038). This work was also partially sponsored by Grant-in-Aid for
359 Scientific Research (Ministry of Education, Culture, Sports, Science and Technology, Japan)
360 (Grant Numbers: 18H01795, 18K18970 and 18K04848). The authors thank Suzukakedai
361 Materials Analysis Division, Technical Department, Tokyo Institute of Technology, for mass
362 spectrometry analysis. In addition, T. K. thanks the Keidanren for the financial supports under the
363 Keidanren Global Fellowship's scheme.

364

365

366

367 **REFERENCES**

- 368 (1) Jenkins, T. F.; Walsh, M. E. Development of Field Screening Methods for TNT, 2,4-DNT
369 and RDX in Soil. *Talanta* **1992**, *39* (4), 419–428. [https://doi.org/10.1016/0039-](https://doi.org/10.1016/0039-9140(92)80158-A)
370 9140(92)80158-A.
- 371 (2) Caygill, J. S.; Davis, F.; Higson, S. P. J. Current Trends in Explosive Detection Techniques.
372 *Talanta* **2012**, *88*, 14–29. <https://doi.org/10.1016/j.talanta.2011.11.043>.
- 373 (3) Håkansson, K.; Coorey, R. V.; Zubarev, R. A.; Talrose, V. L.; Håkansson, P. Low-Mass
374 Ions Observed in Plasma Desorption Mass Spectrometry of High Explosives. *J. Mass*
375 *Spectrom.* **2000**, *35* (3), 337–346. [https://doi.org/10.1002/\(SICI\)1096-](https://doi.org/10.1002/(SICI)1096-9888(200003)35:3<337::AID-JMS940>3.0.CO;2-7)
376 9888(200003)35:3<337::AID-JMS940>3.0.CO;2-7.
- 377 (4) Mullen, C.; Irwin, A.; Pond, B. V.; Huestis, D. L.; Coggiola, M. J.; Oser, H. Detection of
378 Explosives and Explosives-Related Compounds by Single Photon Laser Ionization Time-
379 of-Flight Mass Spectrometry. *Anal. Chem.* **2006**, *78* (11), 3807–3814.
380 <https://doi.org/10.1021/ac060190h>.
- 381 (5) Primera-Pedrozo, O. M.; Soto-Feliciano, Y. M.; Pacheco-Londoño, L. C.; Hernández-
382 Rivera, S. P. Detection of High Explosives Using Reflection Absorption Infrared
383 Spectroscopy with Fiber Coupled Grazing Angle Probe/FTIR. *Sens. Imaging* **2009**, *10* (1–
384 2), 1–13. <https://doi.org/10.1007/s11220-009-0042-1>.
- 385 (6) Pacheco-Londoño, L. C.; Ortiz-Rivera, W.; Primera-Pedrozo, O. M.; Hernández-Rivera, S.
386 P. Vibrational Spectroscopy Standoff Detection of Explosives. *Anal. Bioanal. Chem.* **2009**,
387 *395* (2), 323–335. <https://doi.org/10.1007/s00216-009-2954-y>.
- 388 (7) Zhen, L.; Ford, N.; Gale, D. K.; Roesijadi, G.; Rorrer, G. L. Photoluminescence Detection
389 of 2,4,6-Trinitrotoluene (TNT) Binding on Diatom Frustule Biosilica Functionalized with

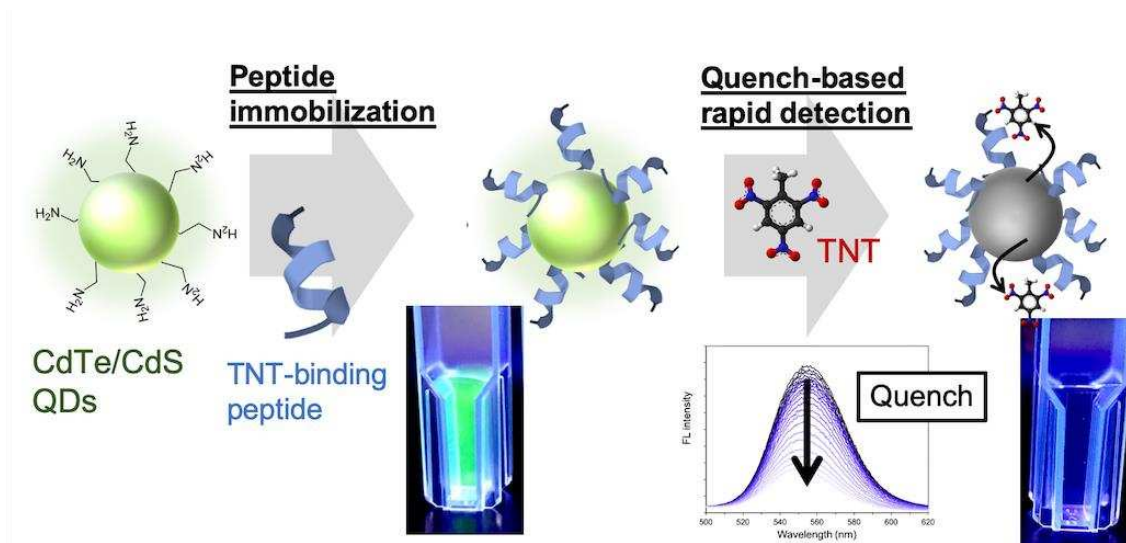
- 390 an Anti-TNT Monoclonal Antibody Fragment. *Biosens. Bioelectron.* **2016**, *79*, 742–748.
391 <https://doi.org/10.1016/j.bios.2016.01.002>.
- 392 (8) Charles, P. T.; Davis, J.; Adams, A. A.; Anderson, G. P.; Liu, J. L.; Deschamps, J. R.;
393 Kusterbeck, A. W. Multi-Channeled Single Chain Variable Fragment (ScFv) Based
394 Microfluidic Device for Explosives Detection. *Talanta* **2015**, *144*, 439–444.
395 <https://doi.org/10.1016/j.talanta.2015.06.039>.
- 396 (9) Liu, J. L.; Zabetakis, D.; Acevedo-Vélez, G.; Goldman, E. R.; Anderson, G. P. Comparison
397 of an Antibody and Its Recombinant Derivative for the Detection of the Small Molecule
398 Explosive 2,4,6-Trinitrotoluene. *Anal. Chim. Acta* **2013**, *759*, 100–104.
399 <https://doi.org/10.1016/j.aca.2012.10.051>.
- 400 (10) Zhang, D.; Jiang, J.; Chen, J.; Zhang, Q.; Lu, Y.; Yao, Y.; Li, S.; Logan Liu, G.; Liu, Q.
401 Smartphone-Based Portable Biosensing System Using Impedance Measurement with
402 Printed Electrodes for 2,4,6-Trinitrotoluene (TNT) Detection. *Biosens. Bioelectron.* **2015**,
403 *70*, 81–88. <https://doi.org/10.1016/j.bios.2015.03.004>.
- 404 (11) Goldman, E. R.; Medintz, I. L.; Whitley, J. L.; Hayhurst, A.; Clapp, A. R.; Uyeda, H. T.;
405 Deschamps, J. R.; Lassman, M. E.; Mattoussi, H. A Hybrid Quantum Dot - Antibody
406 Fragment Fluorescence Resonance Energy Transfer-Based TNT Sensor. *J. Am. Chem. Soc.*
407 **2005**, *127* (18), 6744–6751. <https://doi.org/10.1021/ja0436771>.
- 408 (12) Peveler, W. J.; Roldan, A.; Hollingsworth, N.; Porter, M. J.; Parkin, I. P. Multichannel
409 Detection and Differentiation of Explosives with a Quantum Dot Array. *ACS Nano* **2016**,
410 *10* (1), 1139–1146. <https://doi.org/10.1021/acsnano.5b06433>.
- 411 (13) Xu, S.; Lu, H. Ratiometric Fluorescence and Mesoporous Structure Dual Signal
412 Amplification for Sensitive and Selective Detection of TNT Based on MIP@QD

- 413 Fluorescence Sensors. *Chem. Commun.* **2015**, 51 (15), 3200–3203.
414 <https://doi.org/10.1039/C4CC09766A>.
- 415 (14) Zhu, Y.; Zhang, Y.; Li, N.; Gang, S.; Liu, T.; Bing, N.; Qun, H. A Facile Synthesis of Water-
416 Soluble Carbon Dots as a Label-Free Fluorescent Probe for Rapid, Selective and Sensitive
417 Detection of Picric Acid. *Sensors Actuators B Chem.* **2017**, 240, 949–955.
418 <https://doi.org/10.1016/j.snb.2016.09.063>.
- 419 (15) Han, Y.; Chen, Y.; Feng, J.; Liu, J.; Ma, S.; Chen, X. One-Pot Synthesis of Fluorescent
420 Silicon Nanoparticles for Sensitive and Selective Determination of 2,4,6-Trinitrophenol in
421 Aqueous Solution. *Anal. Chem.* **2017**, 89 (5), 3001–3008.
422 <https://doi.org/10.1021/acs.analchem.6b04509>.
- 423 (16) Hu, Z.; Deibert, B.; Li, J. Luminescent Metal–Organic Frameworks for Chemical Sensing
424 and Explosive Detection. *Chem. Soc. Rev.* **2014**, 43, 5815–5840.
425 <https://doi.org/10.1039/c4cs00010b>.
- 426 (17) Sun, R.; Huo, X.; Lu, H.; Feng, S.; Wang, D. Recyclable Fluorescent Paper Sensor for
427 Visual Detection of Nitroaromatic Explosives. *Sensors Actuators B Chem.* **2018**, 265, 476–
428 487. <https://doi.org/10.1016/j.snb.2018.03.072>.
- 429 (18) Jin, H.; Won, N.; Ahn, B.; Kwag, J.; Heo, K.; Oh, J.-W.; Sun, Y.; Cho, S. G.; Lee, S.-W.;
430 Kim, S. Quantum Dot-Engineered M13 Virus Layer-by-Layer Composite Films for Highly
431 Selective and Sensitive Turn-on TNT Sensors. *Chemical Communications*. 2013, p 6045.
432 <https://doi.org/10.1039/c3cc42032a>.
- 433 (19) Wang, H.; Chen, C.; Liu, Y.; Wu, Y.; Yuan, Y. A Highly Sensitive and Selective
434 Chemosensor for 2, 4, 6-Trinitrophenol Based on L-Cysteine-Coated Cadmium Sulfide

- 435 Quantum Dots. *Talanta* **2019**, *198* (January), 242–248.
436 <https://doi.org/10.1016/j.talanta.2019.02.016>.
- 437 (20) Guo, Z. Z.; Florea, A.; Cristea, C.; Bessueille, F.; Vocanson, F.; Goutaland, F.; Zhang, A.
438 D.; Săndulescu, R.; Lagarde, F.; Jaffrezic-Renault, N. 1,3,5-Trinitrotoluene Detection by a
439 Molecularly Imprinted Polymer Sensor Based on Electropolymerization of a Microporous-
440 Metal-Organic Framework. *Sensors Actuators, B Chem.* **2015**, *207* (PB), 960–966.
441 <https://doi.org/10.1016/j.snb.2014.06.137>.
- 442 (21) Shahdost-fard, F.; Roushani, M. Impedimetric Detection of Trinitrotoluene by Using a
443 Glassy Carbon Electrode Modified with a Gold Nanoparticle@fullerene Composite and an
444 Aptamer-Imprinted Polydopamine. *Microchim. Acta* **2017**, *184* (10), 3997–4006.
445 <https://doi.org/10.1007/s00604-017-2424-8>.
- 446 (22) Tanaka, M.; Minamide, T.; Takahashi, Y.; Hanai, Y.; Yanagida, T.; Okochi, M. Peptide
447 Screening from a Phage Display Library for Benzaldehyde Recognition. *Chem. Lett.* **2019**,
448 *48* (8), 978–981. <https://doi.org/10.1246/cl.190318>.
- 449 (23) Brenet, S.; John-Herpin, A.; Gallat, F. X.; Musnier, B.; Buhot, A.; Herrier, C.; Rousselle,
450 T.; Livache, T.; Hou, Y. Highly-Selective Optoelectronic Nose Based on Surface Plasmon
451 Resonance Imaging for Sensing Volatile Organic Compounds. *Anal. Chem.* **2018**, *90* (16),
452 9879–9887. <https://doi.org/10.1021/acs.analchem.8b02036>.
- 453 (24) Matsumoto, K.; Torimaru, A.; Ishitobi, S.; Sakai, T.; Ishikawa, H.; Toko, K.; Miura, N.;
454 Imato, T. Preparation and Characterization of a Polyclonal Antibody from Rabbit for
455 Detection of Trinitrotoluene by a Surface Plasmon Resonance Biosensor. *Talanta* **2005**, *68*
456 (2), 305–311. <https://doi.org/10.1016/j.talanta.2005.08.054>.

- 457 (25) Okochi, M.; Muto, M.; Yanai, K.; Tanaka, M.; Onodera, T.; Wang, J.; Ueda, H.; Toko, K.
458 Array-Based Rational Design of Short Peptide Probe-Derived from an Anti-TNT
459 Monoclonal Antibody. *ACS Comb. Sci.* **2017**, *19* (10), 625–632.
460 <https://doi.org/10.1021/acscombsci.7b00035>.
- 461 (26) Wang, J.; Muto, M.; Yatabe, R.; Tahara, Y.; Onodera, T.; Tanaka, M.; Okochi, M.; Toko,
462 K. Highly Selective Rational Design of Peptide-Based Surface Plasmon Resonance Sensor
463 for Direct Determination of 2,4,6-Trinitrotoluene (TNT) Explosive. *Sensors Actuators, B*
464 *Chem.* **2018**, *264*, 279–284. <https://doi.org/10.1016/j.snb.2018.02.075>.
- 465 (27) Komikawa, T.; Tanaka, M.; Yanai, K.; Johnson, B. R. G.; Critchley, K.; Onodera, T.; Evans,
466 S. D.; Toko, K.; Okochi, M. A Bioinspired Peptide Matrix for the Detection of 2,4,6-
467 Trinitrotoluene (TNT). *Biosens. Bioelectron.* **2020**, *153*, 112030.
468 <https://doi.org/10.1016/j.bios.2020.112030>.
- 469 (28) Gaponik, N.; Talapin, D. V.; Rogach, A. L.; Hoppe, K.; Shevchenko, E. V.; Kornowski, A.;
470 Eychmüller, A.; Weller, H. Thiol-Capping of CdTe Nanocrystals: An Alternative to
471 Organometallic Synthetic Routes. *J. Phys. Chem. B* **2002**.
472 <https://doi.org/10.1021/jp025541k>.
- 473 (29) Yu, W. W.; Qu, L.; Guo, W.; Peng, X. Experimental Determination of the Extinction
474 Coefficient of CdTe, CdSe, and CdS Nanocrystals. *Chem. Mater.* **2003**.
475 <https://doi.org/10.1021/cm034081k>.
- 476
477

478 TABLE OF CONTENTS GRAPHIC



479

480